Review Article
Open Access
CrossMark

Influence of outdoor conditions on PV module performance – an overview

Abstract

The utilization of renewable sources of energy is of significant interest today. This is particularly the case due to the growing interest in addressing global warming, carbon footprint and the associated challenges for the environment. In this context, the enhanced use of solar panels is relevant and timely. With a view to understand and appreciate the fundamentals of the workings of the solar panels and the influence of the outdoor weather-related parameters on their operational characteristics, a study is presented in this paper. A detailed procedure for performance measurement of PV modules in outdoor conditions is reported. Improvement in the precision of outdoor performance measurements of photovoltaic (PV) modules is investigated for a wide range of outdoor conditions. A comparative performance evaluation of the currently available PV modules under the influence of humidity, irradiance and particle radiation is presented. PV parameters show strong dependence on these outdoor conditions. The instability in solar cell modules when reacting with water or under high humidity inhibits the high performance of solar cell modules. Irradiation results depict that the silicon-based PV modules show a decreasing trend of power conversion efficiency with increasing solar irradiance. The efficiency increases with increased solar irradiance for CdTe, GaAs and CIGS solar cells in the irradiance range of 200 to 1000 W•m^{-2}. Tandem and multi-junction solar cells exhibit a high-power conversion efficiency when the solar irradiance increases from 0 - 70 suns. Perovskite solar cells have better particle radiation tolerance than silicon, III-V and CIGS solar cells. The shading problem is discussed briefly for solar cell modules. This study is aimed to provide valuable and comparable information on the degradation performance of solar cells as function of humidity, irradiance and particle radiation, and serves as the basis for future development.

Keywords: outdoor conditions, PV modules, irradiation, humidity, particle radiation, shaded cell, hot-spots

Volume 7 Issue 2 - 2023

Leqi Lin,[1] Birinchi Bora,[2,3] B Prasad,[3] OS Sastry,[2] S Mondal,[3] NM Ravindra[4]
[1]Department of Civil and Environmental Engineering, New Jersey Institute of Technology, USA
[2]National Institute of Solar Energy, Ministry of New and Renewable Energy, India
[3]TERI University, India
[4]Department of Physics, New Jersey Institute of Technology, USA

Correspondence: NM Ravindra, Department of Physics, New Jersey Institute of Technology, Newark, NJ, USA, Tel 9735963278, Email n.m.ravindra@njit.edu/nmravindra@gmail.com

Received: May 03, 2023 | **Published:** May 19, 2023

Abbreviations: J_{sc}, short circuit of current density; FF, fill factor; Voc, open circuit voltage, P_{CE}, power conversion efficiency; R_s, series resistance; R_{sh}, shunt resistance; I_{scr}, PV module short circuit current at STC; θ, sngle of incidence; δ, declination; φ, latitude; ß, tilt of module; ω, hour angle; Edni, direct normal solar irradiance; E_o, reference global solar irradiance; E_{poa}, global solar irradiance on the plane-of-array (module); AOI, angle between solar beam and module normal vector (degrees); α_{sc}, short circuit current temperature coefficient; I_{sc}, measured short circuit current (A); T_c, measured module temperature (°C); f_d, fraction of diffuse irradiance used by module; SR(λ), relative spectral response of PV module; EAM1.5G, standard AM1.5G spectrum; G_{eff}, effective solar irradiance; P_{max}, maximum power output at maximum power point; MMF, mismatch factor; I_r, rated current; I_m, measured current; V_r, rated voltage; V_m, measured voltage; k, Curve correction factor; α, temperature coefficient of module; I_1 and V_1, pair of measured points on I-V characteristics; I_2 and V_2, pair of points of resulting corrected characteristics; G_1, irradiance measured with reference; G_2, irradiance at reference or other desired conditions; κ, curve correction factor; β, temperature coefficient of V_{oc}; Y_f, final PV system yield; Y_r, reference yield

Introduction

The electricity generation from solar photovoltaic modules will be one of the primary sources of power generation in the near future. Communities from across the world are installing photovoltaic (PV) power plants to feed power to the grid as well as for their own consumption. In general, PV power plants are classified in terms of operating loads and are described in Figure 1. The main components of On-grid power plants are PV modules, inverters, and the electrical grid. On-grid power plant is directly connected to the grid. In on-grid system, consumers are allowed to use part or all of their own generated electricity at any time, instead of when it is generated. They can feed the power to the grid and be compensated for it, thus generating revenue for themselves. Off-grid systems are connected with storage batteries and are used for standalone purposes only. In case of off-grid systems, the solar power is used directly by the load during sunshine period and during no-sun period, load is fed through battery which is charged by the excess power produced during sunshine period. The charging or discharging of the battery is usually controlled by the charge controller. The main components of hybrid system are Power Conditioning Unit (e.g., inverter, Charge controller and data logger), storage battery, PV module, energy meters, transformer and electricity grid. Hybrid system can store energy for the use of consumer and also export all or excess generated electricity.

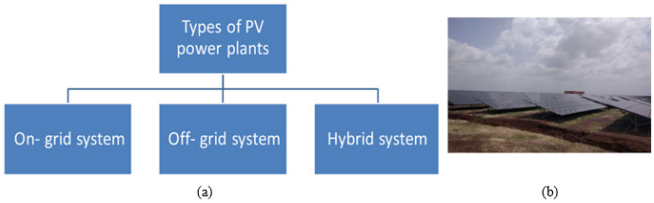

Figure 1 (a) Types of PV power plants, (b) an example of a utility-scale crystalline silicon PV power plant installed over about 8 acres of land.

The outdoor performance of PV module depends on environmental parameters such as irradiance, ambient temperature, humidity, wind

speed and its direction.[1] The performance of PV module with respect to irradiance is not linear for all technologies. The effect of irradiance is mainly on short circuit current and the resulting power output. The module performance also depends on ambient temperature as the PV module temperature depends on ambient temperature. The voltage decreases with increase in module temperature and current increases with it. However, the overall power decreases with increase in temperature. Humidity mainly affects the incident light spectrum and hence the current. Wind speed and its direction affects the module temperature. It has been observed that, with increase in wind speed, the module temperature decreases depending on the season. For example, in some parts of India, during the summer season, hot wind blows during the day time. This increases the module temperature with increase in wind speed.

The performance of PV module is usually tested under indoor conditions, which is referred to as Standard Test Conditions (STC) and Nominal Operating Cell Temperature conditions (NOCT). STC refers to irradiance of 1000 $W \bullet m^{-2}$, module temperature of 25 °C, Air Mass of 1.5, angle of incidence = 0° and NOCT refers to irradiance of 800 $W \bullet m^{-2}$, ambient temperature = 20°C, wind speed of less than 1 $m \bullet s^{-1}$. The prevailing standard for testing of PV modules is IEC 61215.[2] However, as per IEC 61853.[3] the modules are also tested under 22 different conditions of temperature and irradiance.[3] The testing conditions are summarized in Table 1.

Table 1 Testing conditions of PV module as per IEC 61853-1[3]

Irradiance ($W\ m^{-2}$)	Module Temperature (°C)			
	15	**25**	**50**	**75**
1100	NA	1	2	3
1000	4	5	6	7
800	8	9	10	11
600	12	13	14	15
400	16	17	18	NA
200	19	20	NA	NA
100	21	22	NA	NA

For the performance measurements of PV modules in indoor conditions, the following instruments are required: a solar simulator, temperature control unit, light measuring device and a variable electronic load. However, after installation of the PV module in the field, it is neither easy to take the module back to an indoor testing lab for characterization nor is it economical for researchers. Thus, scientists and industry practitioners utilize different performance testing procedures for characterizing PV modules in the field after installation. In this study, a detailed procedure for performance measurement of PV modules in outdoor conditions is reported. It is divided into two sections: (i) Instantaneous performance measurement of PV modules in outdoor conditions and (ii) Long-term performance measurement of PV modules in outdoor conditions. The details of the methodology, required instrumentation, and calculations involved in both the procedures of performance measurements of PV modules in outdoor conditions are presented. Besides, this study presents a comparative performance evaluation of the current commercially available PV modules (e.g., m-Si, a-Si, CIGS, perovskites, tandem, CdTe and GaAs solar cells) under the influence of weather conditions (e.g., humidity, irradiance and particle radiation). An analysis of the effect of humidity and solar irradiance on their output parameters is also presented.

Instantaneous performance measurements of PV modules in outdoor conditions

Equipment required for instantaneous performance testing

Instantaneous performance measurements of PV modules in outdoor conditions are utilized to give rating to the module and to estimate degradation rate after long term of exposure in the field. The required instrumentation to test the instantaneous performance of PV modules in outdoor conditions is described here.

The I-V tracer

The I-V tracer is a device with a variable electronic load to trace the current-voltage curve of a PV module within a fraction of a second. I-V tracer should have a good number of load points to measure the current against the voltage. For drawing I-V curve of an individual module, the current range and voltage measurement range should not be very high compared to module's actual current and voltage values. I-V tracer with a voltage range from 10 V to 1000 V can be used to measure the I-V curve of an individual module and the current range should be within 20-30 A. The uncertainty in measurement of power, current and voltage should be within 1%. It is better to use four wire methods to measure the I-V curve to obtain more accurate results.

Temperature sensor

A temperature sensor is used to check the module temperature during the testing. Usually Pt-100 or Pt-1000 temperature sensors are used because of their accuracy and temperature measurement range. Three sensors are placed in the backside of the module (using conductive aluminum adhesive tape) to get the distribution of temperature when measuring the temperature coefficient of PV module.

Radiation measuring sensor

There are two types of irradiance sensors that can measure the radiation in the plane of the module; these are based on thermopiles and solar cells. Thermopiles can measure irradiance in the wavelength range of 280 nm to 3000 nm. Silicon solar cell-based sensors can measure irradiance in the wavelength range of 300 nm to 1100 nm. For performance measurements of PV modules, usually a silicon solar cell is used as a reference. However, for spectral correction for effective irradiance, Mismatch factor (MMF) can be used for different PV technologies.

Angle of incidence measurement set up

The performance of PV module also depends on the angle of incidence (AOI) of the incident light. With increase in AOI, the effective irradiance decreases and hence the power output. AOI needs to be measured in the plane of the module, as shown in Figure 2a. AOI can be measured with camera or the shadow heights of known object in the same plane. AOI can also be calculated by using theoretical formulae.

Mesh with Different transmissivity

For measuring the performance of a PV module at different irradiance at a fixed temperature, mesh with different transmissivity is required. These sets of data can be used to estimate the series resistance of the module. Mesh greater than the size of the module with 80% and 60% transmissivity is required. There should not be any change in the spectrum of the transmitted light. Proper gap between the module and

Citation: Lin L, Bora B, Prasad B, et al. Influence of outdoor conditions on PV module performance – an overview. *Material Sci & Eng.* 2023;7(2):88–101. DOI: 10.15406/mseij.2023.07.00210

the mesh is required during the testing at different irradiance level. Figure 2b shows the mesh with 60% light transmissivity.

Arrangement for cooling or heating up the PV module

For the measurement of the temperature coefficient of PV module, the module performance needs to be measured at a fixed intensity and different temperatures. The set up should have the facility to cool or heat the PV module beyond the ambient temperature. The module can be situated in an air-conditioned room and the module temperature needs to be controlled to 15 °C. The backside of the module should be insulated; thermocol can be utilized as the insulator on the backside to increase the thermal stability of the module.

Spectro-radiometer

A spectro-radiometer is used to measure the incident light spectrum. The data obtained can be used to estimate the mismatch factor and the effective irradiance of the module. The Spectro-radiometer should be capable of measuring the incident light spectrum in the wavelength range of 280 nm to 1700 nm. Figure 2c shows the Spectro-radiometers installed at fixed tilt equal to latitude.

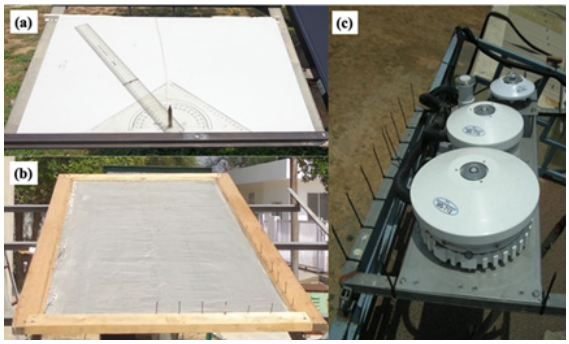

Figure 2 (a) Shadow length measurement set up, (b) Mesh with 60% light transmissivity, (c) Spectro-radiometers installed at fixed tilt equal to latitude.

Procedure for instant performance measurement of PV module under outdoor conditions

Weather check

The irradiance should be more than 800 W•m^{-2} without any rapid cloud movement. A suitable time to perform the measurement is generally between 11:00 AM to 2:00 PM. This can be checked by the irradiance level before and after the I-V curve tracing. The module needs to be cleaned and the I-V tracer be connected before placing the irradiance sensor at the same plane of the module.

AOI correction

For the estimation of Angle of incidence, the real time measured data is used. The angle of incidence can be calculated in the plane- of-module using Equation (1).[4]

$$\theta = \cos^{-1}[\sin\delta\sin(\varphi-\beta)+\cos\delta\cos(\omega)\cos(\varphi-\beta)] \quad \text{Eq (1)}$$

where, θ is the angle of incidence, δ is the declination, φ *is* the latitude, β is the tilt of the module, ω is the hour angle.

The effect of AOI on the performance of PV module needs to be estimated for the distribution of AOI for the entire year. In this section, the methodology reported by King et al is used.[5] *Iscr* is the PV module short circuit current at STC (A); it can be estimated as in Equation (2):

$$I_{sc} = \frac{(I_{sc}\times E_o)}{\left[E_{poa}\times(1+\alpha_{sc}(Tc-25))\right]} \quad \text{Eq (2)}$$

The relative optical response is given by Equation (3):

$$f_2(AOI) = \frac{\left[\frac{(I_{sc}\times E_o)}{\left[E_{poa}\times(1+\alpha_{sc}(Tc-25))\right]}\right]-\left((E_{poa}-E_{dni}\times\cos(AOI))\right)}{\left[E_{dni}\times\cos(AOI)\right]} \quad \text{Eq (3)}$$

where, E_{dni} = Direct normal solar irradiance (W•m^{-2}); E_{poa} = Global solar irradiance on the plane-of-array (module) (W•m^{-2}); E_o = Reference global solar irradiance, typically 1000 W•m^{-2}; *AOI* = Angle between solar beam and module normal vector (degrees); Tc = Measured module temperature (°C); αsc = Short circuit current temperature coefficient (1/°C); I_{sc} = Measured short circuit current (A).

Solar irradiance captured and used by module is known as the effective irradiance. The effective irradiance is technology specific. The effective irradiance due to the *AOI* on the PV module can be calculated using the following formulae, Equation (4):

$$E_e = \frac{\left[E_{dni}\times\cos(AOI)\times f_2(AOI)+f_d\times\left(E_{poa}-E_{dni}\times\cos(AOI)\right)\right]}{E_o} \quad \text{Eq (4)}$$

where, f_d = Fraction of diffuse irradiance used by module, typically assumed = 1.

Spectral correction

If the radiation measuring device requires spectral correction, then the incident light spectrum needs to be measured. By calculating the spectral mismatch factor, the effective irradiance in terms of technology specific spectral content of light can be estimated, as shown in Figure 3. The MMF of a PV technology can be calculated by using Equation (5):[6]

$$MMF = \frac{\int SR(\lambda)E_{AM1.5G}(\lambda)d\lambda}{\int E_{AM1.5G}(\lambda)d\lambda}\frac{\int E(\lambda)d\lambda}{\int SR(\lambda)E(\lambda)d\lambda} \quad \text{Eq (5)}$$

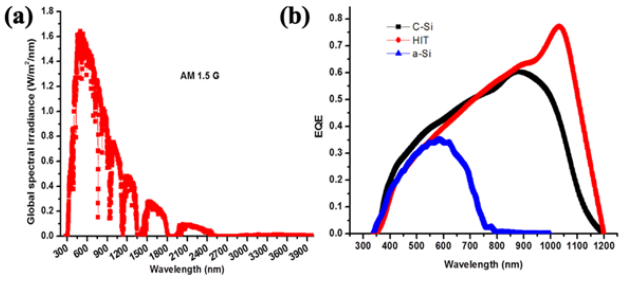

Figure 3 (a) AM 1.5 global spectrum as per IEC 60904-3[7], (b) Spectral responses of PV modules.

where, *SR(λ)* is the relative spectral response of the PV module and *EAM1.5G* is the standard *AM1.5G* spectrum. The effective solar irradiance *(G_{eff})*, corrected by the effect of the solar spectrum, can be calculated by using Equation (6):

$$G_2 = \frac{G}{MMF} \quad \text{Eq (6)}$$

The module needs to be installed facing towards the sun with the angle of incident light as low as possible before placing the irradiance sensor in the same plane of the module.

Temperature coefficient estimation

In order to mitigate the interruption and the generated potential error, the module needs to be cooled before measurement and the temperature sensor must be installed in three different positions on

Citation: Lin L, Bora B, Prasad B, et al. Influence of outdoor conditions on PV module performance – an overview. *Material Sci & Eng.* 2023;7(2):88–101. DOI: 10.15406/mseij.2023.07.00210

the back sheet (top, mid and bottom corner). The data of I-V curve is traced at 15-30 sec at a fixed irradiance and a stabilized module temperature. Normally, the temperature coefficients are measured in terms of I_{sc}, V_{oc}, P_{max}. Other precautions that need to be taken during the measurements include the following: the total irradiance is at least as high as the upper limit of the range of interest; the irradiance variation caused by short-term oscillations should be less than 2% of the total irradiance as measured by the reference device and the wind speed should be less than 2 m•s^{-1}. From this, the variation of I_{sc}, V_{oc}, P_{max} with temperature are obtained, as shown in Figure 4. Subsequently, percentage temperature coefficient is estimated by considering values of I_{sc}, V_{oc}, P_{max} at 25 °C.[2]

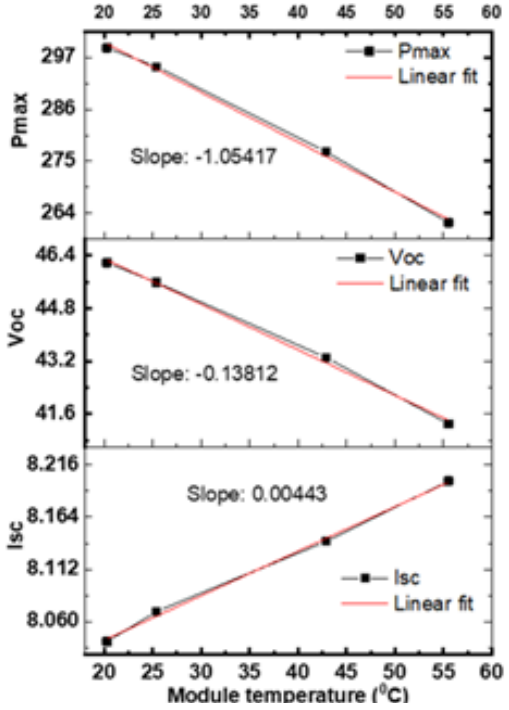

Figure 4 I_{sc},V_{oc}, P_{max} as the function of module temperature.

Series resistance estimation

As per IEC 60891, for the estimation of series resistance, three I-V curves at different irradiance levels with constant temperature and spectrum are required. A mesh is used to obtain different irradiance at the same instant without any change in the incident spectrum and module temperature. In procedure 1 of IEC 60891 method, the current and voltage are obtained from the *I-V* characteristics by using Equations (7) and (8):[8]

$$I_r = \mathrm{I_m} + I_{sc}\left(\frac{G_r}{G_m} - 1\right) + \alpha\left(T_r - T_m\right) \qquad \text{Eq (7)}$$

$$V_r = V_m - R_s\left(I_r - I_m\right) - \kappa I_r\left(T_r - T_m\right) + \beta\left(T_r - T_m\right) \qquad \text{Eq (8)}$$

where, I_r is the rated current, I_m is the measured current, I_{sc} is the short circuit current, R_s is the series resistance, V_r is the rated voltage, V_m is the measured voltage, k is the curve correction factor and α is the temperature coefficient of the module.

The translational procedure 1of IEC 60891 can be mathematically formulated as in Equation (9)-(11):

$$I_2 = I_1 + I_{sc} \times \left(\frac{G_2}{G_1} - 1\right) \qquad \text{Eq (9)}$$

$$V_2 = V_1 - R_s \times \left(I_2 - I_1\right) \qquad \text{Eq (10)}$$

$$P = V_2 \times I_2 \qquad \text{Eq (11)}$$

where, I_1 and V_1 are the pair of measured points on the I-V characteristics, I_2 and V_2 are the pair of points of the resulting corrected characteristics, G_1 is the irradiance measured with the reference; G_2 is the irradiance at the reference or other desired conditions.

For the calculation of series resistance, *I-V* curve at lower radiation with constant module temperature is translated into higher radiation data with the same module temperature. Since *I-V* curves are at the same temperature, temperature coefficient will not play any role. Change in R_s is calculated in steps of 10 - mΩ in the positive or negative direction. The deviation in P_{max} values of the transposed *I-V* characteristics is determined and the proper R_s will be found when the P_{max} deviation is within ± 0.5 % or better,[8] as shown in Figure 5a.

Curve correction factor (κ) estimation

The current-voltage characteristics of the PV module at a constant irradiance and different temperatures covering the range of interest of irradiance condition are traced, which shall not differ by more than ±1 % during the I-V measurements. The *I-V* curve for all the temperatures is translated to the lowest module temperature data by using κ = 0 Ω/K in the translational equation. Starting from 0 mΩ/K, κ needs to be changed in steps of 1 mΩ/K in the positive or negative direction. The proper value of κ is determined when the deviation of maximum output power values of the transposed *I-V* characteristics coincide within 0.5 % or better[8] as shown in Figure 5b.

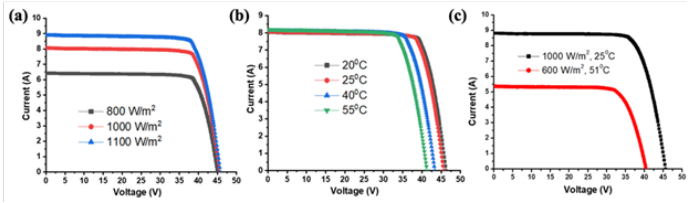

Figure 5 I-V curves of PV module (a) at different irradiance and at same temperature (b) at constant irradiance but different temperatures for estimation of curve correction factor (c) translated I-V curve.

Translation of I-V data to the desired irradiance and temperature condition

Besides the procedure 1 of IEC 60891[2] there are two more procedures in the same IEC standard, which can also be used to translate I-V curve, as shown in Figure 5c. By using equations (12) and (13), the performance of PV module can be estimated at desired irradiance and temperature level. Tables 2 & 3 list the parameters of measured and translated I-V curves.

$$I_2 = I_1 + I_{sc}\left(\frac{G_1}{G_2} - 1\right) + \alpha \times \left(T_2 - T_1\right) \qquad \text{Eq (12)}$$

$$V_2 = V_1 - R_s\left(I_2 - I_1\right) - k \times I_2 \times \left(T_2 - T_1\right) + \beta \times \left(T_2 - T_1\right) \qquad \text{Eq (13)}$$

where, I_2, V_2 are target current and voltage; I_1, V_1 are measured current & voltage; G_2, T_2 are target irradiance and temperature; G_1, T_1 = Measured irradiance and temperature; α is temperature coefficient of I_{sc} (A/°C); β = temperature coefficient of Voc (V/°C); R_s is series resistance (Ω) and κ is Curve correction factor (Ω/°C).

Citation: Lin L, Bora B, Prasad B, et al. Influence of outdoor conditions on PV module performance – an overview. *Material Sci & Eng.* 2023;7(2):88–101. DOI: 10.15406/mseij.2023.07.00210

Table 2 Electrical parameters of measured and translated I-V curves

Conditions units	I_{sc} A	I_{mmp} A	Vo_c V	V_{mmp} V	P_{max} W	FF %	R_s Ohm
Measured at 600 W m^{-2}, 51 deg C	5.36	5.09	40.46	32.22	164.07	75.64	0.841
Translated to 1000 W m^{-2}, 25 deg C	8.81	8.43	45.63	36.3	306.14	76.14	0.583

Table 3 Maximum power (W) of a m-Si module as a function of irradiance and temperature as per IEC 61853-1

Irradiance W m^{-2}	Spectrum	Parameter: Maximum power (P_{max})			
		15°C	25°C	50°C	75°C
1100	AM1.5	NA	323.76	297.01	265.33
1000	AM1.5	303.74	295.06	270.77	243.03
800	AM1.5	240.66	233.35	212.56	194.42
600	AM1.5	178.76	173.29	158.76	146.12
400	AM1.5	115.99	113.2	103.48	NA
200	AM1.5	54.89	54.01	NA	NA
100*	AM1.5	25.84	25.59	NA	NA

Long term performance measurement of PV module under outdoor conditions

Weather station system

For long term performance evaluation of PV module in outdoor conditions, continuous measurement of weather parameters and performance of PV module is required. The height of the weather station is the same as the height of the equipped PV test bed to collect the data. The interval for weather data recording should be less than 5 minutes to capture the variations properly. For continuous performance measurements of PV modules, different types of test beds are designed. In this section, two different types of measurement set up are explained, which are test bed with I-V tracer and test bed with Inverter. Table 4 summarizes the measured weather parameters and the instruments that are used for the measurements.

Table 4 List of weather parameters to be measured and instruments required

Parameter	Instrument
Global irradiance in plane to the module surface and at horizontal surface (0-1400 W m^{-2})	Pyranometer (Thermopile or silicon solar cell based)
Direct normal irradiance (0-1400 W m^{-2})	Pyrheliometer
Spectrum (Wavelength: 0.28 to 1.7 µm)	Spectroradiometer
Ambient temperature (-40 to +60 °C)	Digital Thermometer
Wind speed and direction (For wind speed 0-99 mph, For wind direction 0 - 359o)	Anemometer/ wind monitor
Atmospheric pressure (500 -1100 hPa)	Barometer
Rain (0 - 9999 mm)	Rain Gauge
Humidity (10 - 100%)	Humidity probe
Angle of incidence of Sun light (-90 to +90o)	Sensor for angle of incidence

Test bed with I-V tracer

Two types of exposure procedure can be used in the reliability testing of module using *I-V* tracer, as shown in Figures 6a & b. The first, module exposure test, is that in which each module is exposed without loads, and the other, system exposure test, is that the array consisting of several modules is exposed under Maximum power point tracking (MPPT) control with loads. In each procedure, I-V characteristics of the modules and that of the array are measured in a certain interval (five to ten minutes). In the module exposure test, modules are in loaded condition during stand-by condition. The modules are connected to the load in parallel. In the system exposure test, the operating current, under MPPT control, flows in the modules during the stand-by condition, and it is a condition similar to when the modules are actually used. Moreover, in the system exposure test, the string voltage potential should be similar as they are used in the MWp (Megawatt peak) scale power plants. It may cause potential induced degradation in the system exposure test. The procedure for the system exposure test has the possibility to cause failures such as hot-spots, insulation failure and delamination rather than those due to module exposure test.

In grid connected system, the power conditioning system is connected which can control the MPPT and grid connection. In case of stand-alone measurement system, the PV array is MPPT controlled by MPPT unit and the power is stored in battery during stand by condition by the charge controller. The power stored in the battery is used for the measurements. If the power exceeds the battery capacity, the excess power will be consumed by the electrical load.

Test bed with inverter

In case of test bed with inverter module, it can be exposed in both ways. In case of system exposure, the array of several modules is connected to the inverter as connected in a power plant, as shown in Figure 6c. The inverter should be MPPT operated. The string voltage of the module should be similar as in use. Megawatt power plants can also be used as a test bed if the system voltage needs to be maintained. The measurement of maximum current and voltage can be done with the help of MPPT controller within certain interval of time (6 times a second). For the measurement of short circuit current and open circuit voltage, usually two reference modules are used with relay. This can be named as module exposure test. The maximum current and voltage measurement can also be performed with the help of MPPT controller. The MPPT samples the output of the PV modules and selects the most appropriate operating point to obtain maximum power under the prevailing environmental conditions. The PV performance data collected should include the MPPT efficiency. Operational data needs to record for a sufficient period of time to allow the PV modules to complete any initial light induced degradation, and to collect a minimum of one year of operation data in order to visualize the impact of seasonal weather variation on each PV system.

Citation: Lin L, Bora B, Prasad B, et al. Influence of outdoor conditions on PV module performance – an overview. *Material Sci & Eng.* 2023;7(2):88–101. DOI: 10.15406/mseij.2023.07.00210

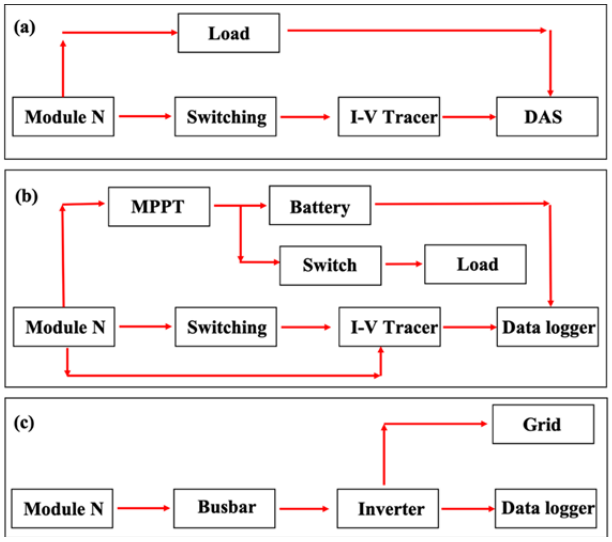

Figure 6 (a) Grid connected power plant with I-V tracer (b) Grid connected power plant with I-V tracer and Battery connected power plant with I-V tracer (c) Grid connected PV power plant with inverter.

Performance indices of PV power plant

Performance ratio (PR)

Long-term performance evaluation and degradation rate of PV power plant performance ratio involve the use of capacity utilization factor. The performance ratio (PR) represents the performance of the PV modules at outdoor conditions compared to their performance under STC, as in Equations (14)-(16), which is calculated as the final PV system yield, Y_f, divided by the reference yield (Y_r). PR depends mainly on the module temperature. For reducing the seasonal effect and temperature effect, PR should be normalized with respect to temperature. This can be estimated by normalizing the instant output to 25°C from the measured module temperature using the power temperature coefficient. Temperature normalized power can be estimated by using following Equations (14) and (15).

$$PR = \frac{Y_f}{Y_r} \quad \text{Eq (14)}$$

where Y_f (Dimensionless quantity) is the final PV system yield, Y_r is the reference yield.

$$Y_f = \frac{E}{P_o} \quad \text{Eq (15)}$$

where the PV system yield (Y_f), (kWh/kW) or (hours) is the net energy output E divided by the D.C. power (P_o) of the installed PV array.

The reference yield (Y_r), (hr) represents an equivalent number of hours at the reference irradiance. It is a function of the location, orientation, and tilt angle of the PV array, and changes from day-to-day, month-to-month and year-to-year with weather variability:

$$Y_r = \frac{H_t}{G} \quad \text{Eq (16)}$$

where the reference yield, (hr) is the total in-plane solar insolation (kWh) divided by the PV's reference (STC) irradiation (kW).

PR depends mainly on the module temperature. For reducing the seasonal effect and temperature effect, PR should be normalized with respect to temperature. This can be estimated by normalizing the instant output to 25°C from the measured module temperature using the power temperature coefficient:

$$P_{norm} = P + (T_m - 25) \times \gamma \quad \text{Eq (17)}$$

where, P_{norm} is the normalized power, T_m is the module temperature and γ is the power temperature coefficient.

The total energy is estimated by summing up the normalized power for the desired interval. The total energy needs to be estimated by summing up the normalized power for the desired interval as in Equation (18).

$$E = \sum P_{norm} \quad \text{Eq (18)}$$

Capacity utilization factor (CUF)

CUF is the ratio of the energy output from a solar PV plant over the time of interval to the maximum possible output from it for the same interval of time under ideal conditions.

$$CUF = \frac{Total\ energy\ output\ for\ the\ desired\ time\ period\,(kWh)}{Installed\ plant\ capacity\ (kW) \times 24hr \times Time\ period\,(days)} \quad \text{Eq (19)}$$

In general, CUF of a PV power plant varies from 15 to 20% and it depends on the climatic conditions at the site. In case of concentrator PV system, a maximum of around 35% CUF is observed in the field.

Data analysis tools and performance index for PV power plants

The software should consist of programming for sensing weather sensors, estimating, averaging, integrating and tabulating weather parameters, as shown in Figure 7. The embedded device collects all the data from weather sensors, forms tables in database using MySQL freeware database package. It is possible to create CSV files containing individual table, as well as the entire database. The data can be collected over wide range of time and data for specific period and can be easily selectable for specific period. Software also includes program for I-V measurements of PV arrays and modules versus time. The data is collected for the entire 24 hours. The heart of the data logging facility is the timestamp facility, to help the user to view and compare I-V curves over selected time period for different technology modules. This is achieved by using indexing feature of database tables, so that the insertion and retrieval of data can be fast, even if the span of data is between years. It is estimated that, for a day, about 230 KB are required for weather data and about 3 MB is required for storing PV monitoring data for one technology per day.

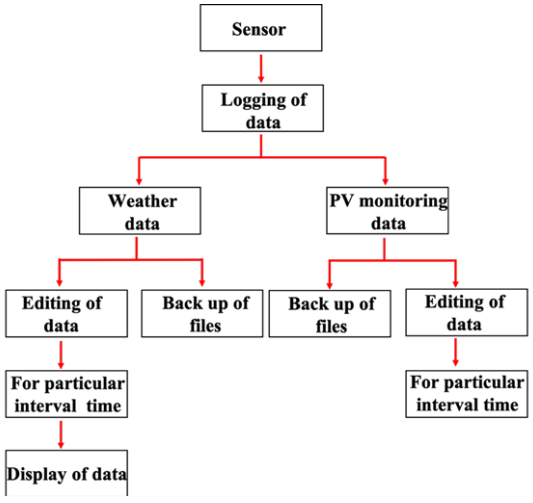

Figure 7 Flow chart of data collection.

Citation: Lin L, Bora B, Prasad B, et al. Influence of outdoor conditions on PV module performance – an overview. *Material Sci & Eng.* 2023;7(2):88–101. DOI: 10.15406/mseij.2023.07.00210

Besides, the reliability of the system should be high enough to operate in harsh environments. The design should support high channel to channel isolation, noise rejection, low-cost, high-density I/O, analog, digital modules, surge suppression and signal conditioning. Moreover, the installation and expansion should be done easily. For the analysis of data of PV modules, the software should be able to estimate series resistance, curve correction factor and translation of I-V data to desired irradiance and temperature conditions.

Degradation rate estimation of PV module

Degradation rate can be estimated by using equation (20).

$$\text{Percentage of degradation} = \frac{(initial\ P_{\max} - Final\ P_{\max}) \times 100\%}{initial\ P_{\max}} \quad \text{Eq (20)}$$

There are different methodologies for estimating the degradation rate. It can be determined by both continuous and discrete data sets. In case of continuous data category, the degradation rate can be calculated by using performance ratio or by using the energy estimation method such as PVUSA. Figure 8 show the distribution of instant degradation rate of PV modules in a power plant in India after 3 years of operation and distribution of PR in a year of three different technologies.

Figure 8 (a) Distribution of instant degradation rate of PV modules in a power plant in India after 3 years of operation and Figure 8(b) Distribution of PR in a year of three different technologies.

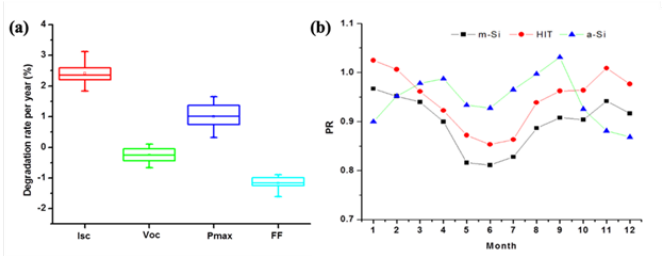

Figure 8 (a) Distribution of instant degradation rate of PV modules in a power plant in India after 3 years of operation and (b) Distribution of PR in a year of three different technologies.

Influence of weather conditions on the solar cell module efficiency

Effect of irradiance

Various researchers and scientists have worked on the performance evaluation of photovoltaic systems under different weather conditions. The efficiency performance for outdoor is different from that of STC since there are many factors (e.g., humidity, irradiance and particle radiation) which may affect the efficiency for outdoor conditions. The influence of temperature on the efficiency performance of solar modules has been reported in the literature.[9] Buday et al.,[10] found out that CIGS modules demonstrated linear increase in P_{max} and J_{sc} ; *FF* and V_{oc} show a rapid increase from dark condition to light condition and undergo a steady but gradually decreasing trend after 600-800 W•m^{-2} over a full range of increasing irradiance, as shown in Figure 9. In Figure 10, the new generation solar cell modules, such as CIGS, (dye-sensitized) DSC and (organic thin film) OPV, show that the efficiency and *FF* decrease when the irradiance increases from 200 to 1000 W•m^{-2}, which may be ascribed to the variation of series resistance in these thin film solar cells.[11] V_{oc} increases with increasing irradiance due to high photo-generated current density. In Figure 11, comparing the performance of PSC-2019-Tress and HIT-2019-Tress regarding the irradiance dependence of the *PCE*, it is observed that the performance of PSC-2019-Tress decreased less than that of HIT-2019-Tress. This is due to the higher V_{oc} of PSC-2019-Tress than that of HIT-2019-Tress, leading to smaller relative changes in *PCE* when the V_{oc} decreases by a constant value, and the larger V_{oc} is ascribed to larger E_g of PSC. Besides the HIT and PSC devices, the performance of silicon-based devices (e.g., m-Si, p-Si and c-Si), especially a-Si device shows a decrease in performance in the irradiance range of 500-1000 W•m^{-2}, in which most electricity is produced. However, for the thin film and III-V solar cell devices, such as GaAs, CIGS, CdTe and AlGaAs/InP/Ge, they have a higher efficiency at high irradiance. It is also reported that tandem cell and multi-junction layer devices, such as perovskite/c-Si and AlGaAs/InP/Ge have higher PCE as the irradiance increases from 1 sun to at least 70 suns, which is ascribed to their larger Eg and higher long-term thermal stability. Different light intensity not only changes the photo-generated current density, but also has a significant impact on the PV parameters, such as R_s, R_{sh}, *FF*, diode ideality factor A and reverse saturation current density.[12]

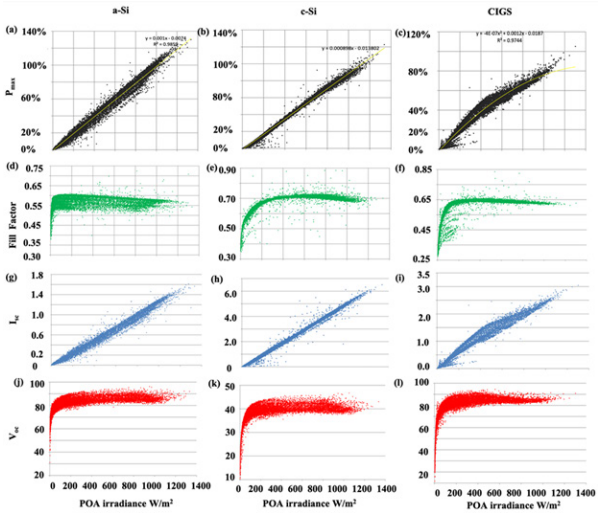

Figure 9 a-Si, c-Si and CIGS module (a)-(c) P_{max} , (d)-(f) fill factor, (g)-(i) I_{sc} and (j)-(l) V_{oc} versus intensity of light (POA Irradiance) in the range of 0-1400 w/m^2 in Taxila, Pakistan. The figure is regenerated from Ref.[10] with permission.

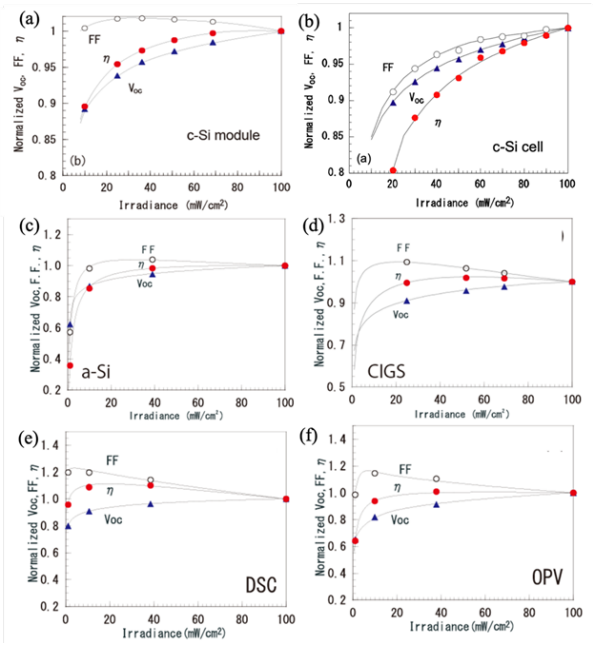

Figure 10 PV parameter performance under irradiation range of 0-100 mW/cm^2 for different solar cell and modules, such as (a) c-Si module, (b) c-Si cell, (c) a-Si, (d) CIGS, (e)DSC and (f) OPV. The figure is regenerated from Ref.[11] with permission.

Citation: Lin L, Bora B, Prasad B, et al. Influence of outdoor conditions on PV module performance – an overview. *Material Sci & Eng.* 2023;7(2):88–101. DOI: 10.15406/mseij.2023.07.00210

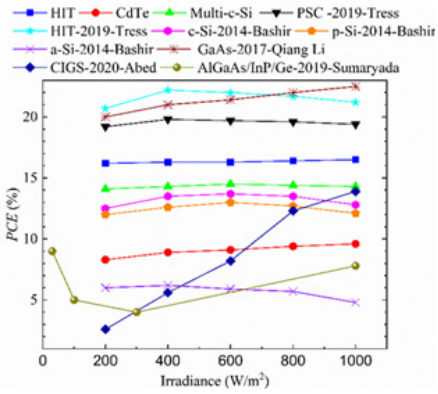

Figure 11 Variation of *PCE* with irradiance - for different solar cell devices; the data is extracted from Ref.[12,13]

Effect of humidity

Besides the influence of irradiance, PV module performance is sensitive to humidity; in general, it is anticipated that moisture will lead to oxidation and instability in materials and devices, leading to the degradation of the device eventually. Thus, the influence of humidity on solar cell performance is a key factor to consider, especially in outdoor conditions. The relative humidity (RH) varies with respect to water vapor saturation pressure and is mainly affected by temperature. For PSCs, the degradation is ascribed to the hydrolysis reaction, in which the organic species in the perovskite decomposes resulting in the release of gas phase HI and CH_3NH_2 when reacting with water.[14] It has been observed that when the PV module is exposed to high RH conditions, the water will penetrate into the solar cell which leads to the delamination and corrosion of the encapsulant,[15] as shown in Figure 12. Panjwani et al.,[16] reported that the humidity brings down the utilization of solar energy from 70% to 55-60% of utilized energy from the sun. Mekhilef et al.,[17] also reported a decrease in cell performance with increasing relative humidity in a-Si module, as shown in Figure 13a. This may be due to the refraction and reflection of irradiance from the water molecules. The PV modules showed high efficiency at low RH, which implies that high RH adversely affects the performance of PV parameters.[18] In Figure 13b, p-Si module exhibits a sharper decrease than that of a-Si and m-Si in both I_{sc} and P_{max} . This indicates that the performance of p-Si module is more sensitive to the variation in humidity. Besides the silicon based PV modules, for thin film solar cells and tungsten-based cells, PV parameters (e.g., P_{max}, V_{oc} and J_{sc}) decrease with the increasing RH, as shown in Figure 13c & 13d. The high RH also facilitates the growth of fungi and other algae, which will possibly accelerate the degradation of solar cell devices.[19]

The figure is regenerated from Ref.[15]with permission.

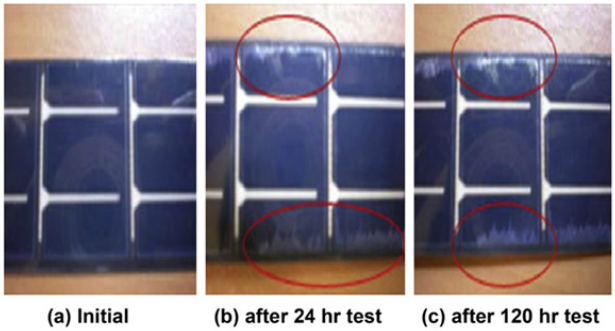

Figure 12 The encapsulant delamination of solar cell device after 24, 120 hours' humidity test. The figure is regenerated from Ref,[15] (With permission).

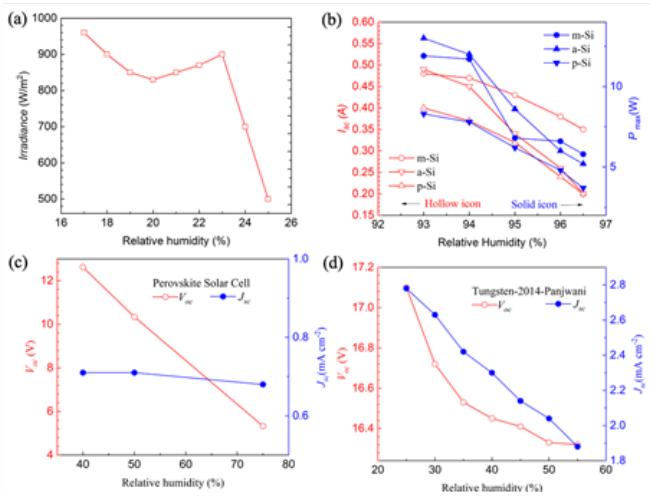

Figure 13 (a) RH- irradiance relations in the low relative humidity range for a-Si module, the figure is regenerated with the permission from Ref.[15]. (b) I_{sc}-Relative humidity-P_{max} relation for high humidity for m-Si, a-Si and p-Si modules. The data is extracted from Ref.[20] . (c) V_{oc}-*RH*-J_{sc} for perovskite solar cell and (d) for tungsten-based cell - data extracted from Ref. [21] and [16] respectively.

Effect of particle radiation

In the wavelength range of 250-2500 nm, the visible range has the highest energy density; therefore, the materials of interest for solar cells should have the capacity to absorb the visible light.[17] In space, there are two types of solar radiation which will affect the performance of solar cells: particle radiation (alpha-rays, protons, and electrons) and wave radiation (gamma-ray).[22] Radiation induced defects increase the localized states within the band gap and hence increase the recombination probability in solar cells.[23] Thus, only materials with high radiation tolerance can be used to fabricate solar cells that are designed for use in space applications. Currently, III-V compounds - based solar cells exhibit better radiation tolerance and offer significant reliability among solar cells in space. Hybrid perovskite solar cells show the potentiality as lightweight, flexible and low-cost materials to hold excellent radiation tolerance as well for space use.[24] CdTe based solar cells are suitable for space applications due to their economic advantages, relatively simple process, and high specific power relative to their thinness.[25]

The other factor which is defined as the ratio of the degraded value to the initial value is used to assess the degradation mechanism of PV parameters. Particles with sufficient energy to completely penetrate the active region of the solar cell produce a roughly uniform damage concentration along their path.[26] However, particles with lower energy that come to rest inside the solar cell create an inhomogeneous defect distribution. In the case of protons, the displacement rate (displacement/cm) increases significantly with decrease in energy, producing highly uniform defect profile wherein most of the damage is concentrated near the end of proton trajectory.[27] In 2019, Lang et al.,[28] investigated perovskite solar cells under proton radiation induced current with 68 and 20 MeV and a total dose in the range of 10^{11}-10^{12} protons•cm^{-2}. The result shows a better radiation hardness than SiC and maintain 95% of the initial *PCE* after proton radiation energy of 68 MeV at a total dose of 10^{12} protons•cm^{-2}, which is ascribed to the role of iodine related defect states. Figure 14 shows the performance of solar cells made from various semiconductors when exposed to proton irradiation. In general, CdTe (proton energy of 100 MeV) and FAMAPbI3 (proton energy of 68 MeV) exhibit low degradation after high dose of proton particle-fluence (10^{15} p•cm^{-2}) which exceeds three

Citation: Lin L, Bora B, Prasad B, et al. Influence of outdoor conditions on PV module performance – an overview. *Material Sci & Eng.* 2023;7(2):88–101. DOI: 10.15406/mseij.2023.07.00210

times the damage threshold of c-Si. Moreover, perovskites, when combined with CIGS, retain over 85% of the initial efficiency under high dose of proton particle- fluence (2 x 10^{12} p•cm^{-2}) and high proton energy (68 MeV), which is comparable to conventional GaInP/ GaAs/ Ge.[29] The results of the J-V curves show that the radiation induced loss originates from the reduction in V_{oc} and *FF;* however, the J_{sc} remains high. In contrast to perovskite/SHJ tandem solar cells, the efficiency decreases drastically under the same proton particle-fluence and energy, which mainly comes from the proton-irradiation-induced trap states from a low radiation-hard bottom cells. Thus, the improvement in bottom cell with high radiation-hardness is useful to mitigate the loss of V_{oc}; subsequently, perovskite based tandem solar cells, with high radiation-hard bottom cells, have the potential to become a disruptive space PV technology.

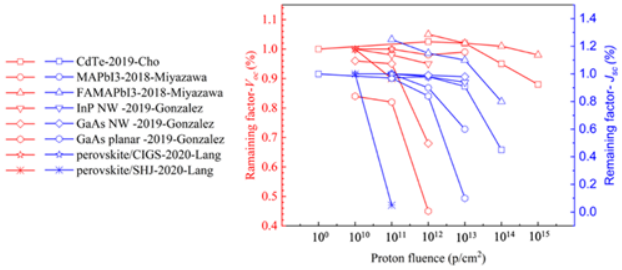

Figure 14 Remaining factors of V_{oc} and J_{sc} as a function of proton fluence for various solar cells under different proton energy: CdTe (100MeV), $MAPbI_3$ (68MeV), $FAMAPbI_3$ (50keV), InP NW, GaAs NW and GaAs planar (350keV) and perovskite/CIGS and perovskite/SHJ (68MeV). The data is extracted from Ref.[29,31,33]

Generally, the electron radiation tolerance of solar cells increases with a thinner light absorber, which has higher optical absorption coefficient, and the displacement rate (displacement/cm) decreases gradually as they are slowed down in the semiconductor. In Table 5, the electron radiation tolerance of solar cells, made from different semiconductors, is summarized. Perovskites have better electron tolerance than silicon, III-V multijunction and CIGS - based solar cells. Among the III-V solar cells, free standing GaAs vertical configuration performs better than planar configuration, and is more suitable for application in space.[30] The combination of thin film materials and large carrier diffusion length of the perovskites (>1 mm) is advantageous for higher radiation tolerance; this is due to the photogenerated carriers in the presence of radiation-induced defects and traps and have sufficient diffusion to contribute to power generation.[31] The low Jsc for CdTe is due to the electron irradiation generated heat, resulting in the diffusion of copper ions, which leads to decrease in minority carrier lifetime.[32]

Approaches to hot-spot reduction and shade loss minimization

Shaded cell loss and hot-spot heating

Apart from the influence of weather conditions on solar cell performance as was discussed previously, it is critical to investigate the performance and stability of solar cell modules, especially shadow loss, which is partial electrical mismatch. Shadow loss effect of the solar cell module is an important consideration in the application of solar cells as power supplies for satellites. Several solar cells, among whole PV module, can be shaded due to fallen leaves, dust accumulation, animal activity and other obstacles that lead to non-uniform power generation, or when there is intrinsic difference between each solar cell. The amount of power loss is a function of the size and shape of the shadow, the geometrical and electrical layout of the cells in the string, and the way the shadow falls across the particular solar cell module.[40] A PV module is a series-connected string of cells, and all the cells must conduct the same amount of current. The PV module system carries the same current even when some of the solar cells are shaded; therefore, the shaded cells behave like a reverse-bias diode.

Table 5 Comparison of electron beam (EB) tolerance of different semiconductor solar cells after exposure to a 1MeV with total dose of 1x1016 Particle.cm^{-2}

Ref.	31	34	35	36	37	38	39	30
	MAPbI3	FAPbI3	c-Si	InGaP/InGaAs/Ge	CIGS	CdTe	GaAs planar	GaAs vertical
	Remaining factor (%)							
J_{sc}	98	100	80	82	99	62	48	95
V_{oc}	97	90	80	82	99	96	83	90
FF	96	92	93	92	99	98	--	--
P_{max}	92	--	60	62	--	--	40	--
P_{CE}	--	94	--	--	99	59	--	--

Moreover, hot-spot heating occurs when there is one or several shaded cells among a large number of cells in string, which causes reverse bias across the shaded cell.[41] This phenomenon contributes to large dissipation of power in the shaded cells. When a solar cell reaches the breakdown voltage, the cell is damaged permanently. IEC 61215 defines and verifies the hotspot tolerance of a solar cell module by a hotspot endurance test. Hot-spot temperature of opaque PV modules is higher than semitransparent cell by 2–3 °C under STC.[42]

The solar cells have a breakdown voltage where the corresponding current turns into reverse bias. Silicon cells generally breakdown in reverse bias by avalanche breakdown (>15V); CIGS and CdTe cells exhibit breakdown voltage < 10 V and a decrease in breakdown voltage under illumination.[43] PSCs have much lower breakdown under reverse bias than crystalline silicon and inorganic thin-film solar cells; this occurs between -1 to -4 V.[43] By performing experiments, Yang et al.,[44] proposed that reverse current should be less than 1.0A for monocrystalline-Si solar cells when the reverse bias is less than -12V. Bowring et al.,[44] reported the mechanism of reverse bias degradation for perovskite solar cell in dark (long time shading), in which current flows in reverse bias most likely due to tunneling mediated by mobile ions. Both the R_s and breakdown voltage increase and V_{oc} decreases under this condition. However, even this degradation in efficiency is recoverable; it takes longer and longer time to recover after each shading event. As a result, the study proposed two options to address the shading induced degradation problems - one involves designing thin cells that breakdown at lower voltage to reduce dissipation of power. Another is to design cells with larger breakdown voltage with bypass diodes.

Minimization and prevention of shaded cell and hot-spot loss

In order to prevent hotspot failure, a passive bypass diode protection device on the solar cell module is mounted. Recent

state-of-the-art technologies on the investigation of effect of shade loss and hot-spot problem are categorized into five types: Partially shading,[45] which revisits and estimates the effect of shading on the PV module; Field test, which analyzes the performance of PV module under real condition in a specific period; Bypass diode topology, which investigates the impact of diode arrangements within the solar cell module; Artificial intelligence, which models and predicts the performance of solar cell module under specific conditions and new mitigation technologies, which search for new technology to mitigate or solve the shading problem.

Bypass diode,[46] as the primary method to address the shade loss problem, provides the bypass path for the current flow; thus, the generated power will not affect the shaded cell. However, the activated bypass diode brings the inevitable voltage drop and consumes the generated power. Thus, it affects the maximum power delivered by the solar cell modules.[47] Mostly, the bypass diodes should have forward voltage as low as possible (e.g., Schottky diode). However, a lower forward voltage means a higher leakage current, raising the risk of thermal runaway.[48] Thus, the bypass diodes must conduct when one cell is shaded, and the shaded cell must be operating under its breakdown voltage.[48] In 2018, Shin et al.,[49] studied the effect of operating conditions on the photovoltaic parameters of installed bypass diode on the back side of PV module in a closed junction box. The result gives insight into an easy heat dissipation and leakage current monitoring method under high temperature when designing a bypass diode junction box.

The configuration of bypass diodes on PV modules, forming part of the array, has an important influence on the possibility of presence of hotspots.[50] In order to determine the shading pattern of PV modules, experimental investigations are needed on a given array size under different shaded conditions. In 2017, Bana et al.,[51] investigated the effects of uniform shading on m-Si PV modules to obtain the output performance and analysis of results under real operating conditions for possible shading scenarios. Prevention is better than cure; thus, it is necessary to establish a flexible inspection scheme, cleaning plan and utilizing data science technologies to reduce the risk of fire under various weather conditions. In 2018, Kaid et al.,[52] proposed a surveillance approach based on the failure diagnosis of PV modules using an adaptive neuro-fuzzy inference approach, which allows early defect identification of the shading cell. Moreover, in 2019, Khan Niazi et al.,[53] using machine learning based on Naïve Bayes classification on the thermal images of PV modules, effectively and rapidly detected, evaluated and categorized failure conditions for PV modules. This machine learning based monitoring method achieved an accuracy of 94.10% with low computational cost.

In 2017, Dhimish et al.,[54] designed a two hot-spot mitigation technology which is capable of enhancing the output power of PV modules under hot-spot loss and shading conditions. This technology adapts two connected integration MOSFETs with the affected PV module, which is observed to increase the output power by 1.44 W and 3.97 W via two hot-spot mitigation techniques, respectively. Furthermore, in 2019, Dhimish et al.,[55] proposed a current limiter circuit to overcome partial shading and hot-spot loss conditions by decreasing its temperature level from 21.3 to 16.4ºC. In 2023, Afridi et al.,[56] investigated the stress endurance of two monocrystalline modules with a half-cell glass/backsheet (G/B) module and a full-cell glass/glass (G/G) module. The results show that the G/G module reached a maximum temperature of approximately 200 °C for a cell shading of 25 %, 55 °C higher than the maximum hotspot temperature of 145 °C in the G/B module, which indicates that half-cell design could minimize the hotspot degradation in crystalline silicon based solar cells.

Concentrated solar power

Current technologies and state-of-the-art energy storage materials

Concentrated solar power (CSP) systems convert the incident solar energy to electricity by using mirrors or lenses to concentrate sunlight energy onto a receiver to drive steam turbines or engines. There are several CSP technologies including linear Fresnel reflector, central receiver (power tower), parabolic dish/engines systems and parabolic trough system,[57] as shown in Figure 15. Most of the CSP systems operate with heat transfer liquid (HTL) and thermal energy storage system (TES) as power plants to provide continuous electricity, irrespective of day or night, which is one of the best candidates as the replacement for combustion of fuel sources for sustainable development. It has been reported that the global CSP market size was valued at US$ 4.5 billion in 2019 and is expected to grow at a compound annual growth rate (CAGR) of 9.7% from 2020 to 2027.[58] With a mission to address climate change in and around the developed and developing countries and the crisis of fluctuation of fuel oil price, CSP offers great promise of green and low-cost energy compared with conventional fuel combustion plants, especially for tropical countries with vast area.

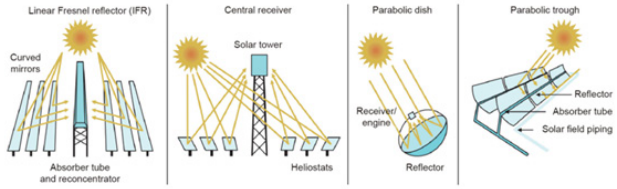

Figure 15 Concentrated Solar Power Systems.[59]

Parabolic trough has easier construction and maintenance among all types of CSP in which countries such as Spain has the highest number of parabolic troughs followed by the U.S.A. and China. Linear Fresnel reflector and Parabolic trough are both linear focusing systems while the other two are point focusing types, which can produce solar heat at higher temperature due to the higher sunlight concentration ratio.[59] The central receiver solar tower type is considered as the most potential one due to its higher efficiency of ~ 18%, [60] and is expected to be the first priority for many countries for the construction and adoption of CSP. The typical Parabolic dish system is composed of a parabolic concentrator connected with a receiver and an alternator. Currently, the overall efficiencies of 13%- 32% and 1.0 kW- 38.8 kW power are generated from parabolic dish type CSP depending on the differences in size, design and radiation utility. The highest efficiency of 29.4 % with 25.3 kW have been reported by Boeing, in California, USA while the reported maximal theoretical efficiency was 32% in a lab study.[61] It is also highlighted that the hybridization mode of CSP with the cooperation of crops, water desalination, thermal storage and solar cooking makes widespread application for CSP.

Normally, the commercial molten salt for TES is a non-eutectic salt mixture of $NaNO_3$/KNO_3. with the limitation of material thermal decomposition temperature of around 565ºC. $MgCl_2$/KCl/NaCl is still considered to be the most promising chloride salt mixture. This thermal decomposition temperature further limits the maximum heat storage capacity. Thus, advanced improvement in the efficiency can be achieved by operating TES system with higher thermal stability. NREL proposed one of the novel molten salt, TES/HTF system,

Citation: Lin L, Bora B, Prasad B, et al. Influence of outdoor conditions on PV module performance – an overview. *Material Sci & Eng.* 2023;7(2):88–101. DOI: 10.15406/mseij.2023.07.00210

with the operating temperature of 520-720°C combining with a supercritical carbon dioxide (sCO_2) Brayton power cycle (operating temperature 500-700°C), which can have energy efficiency higher than 50%.[62] Four main kinds of promising technical concepts have been researched intensively including solid particles as TES/HTF, molten salts (especially chlorides) as TES/HTF, gases as HTF (e.g., helium) with indirect TES (e.g., solid media, PCMs), and liquid metals as HTF with different TES options (e.g., PCMs).[59] Future work will target on the mitigation of the corrosion problem and the thermal durability of molten salts than focus on scaling up issues from the laboratory to commercial scale.

Agri-photovoltaics

With continued progress in technologies and the improved quality of life around world, the demand for electricity has increased significantly. The decreasing mortality and the increasing population have also led to the increasing demand on food worldwide. Thus, we are in the nexus of the land area for food and energy (economy and technology). Solar photovoltaics, as one of the most environmentally friendly and feasible green energy generation sources, copes with climate change and global warming, and is encouraged by many countries. The market for large area of land and concentrated solar power systems is also increasing with land scarcity. Thus, it is critical to address the issues of land utility for concentrated solar power systems especially with regard to the potential distribution of land for grazing and agriculture use. Consequently, agri-photovoltaics provides the benefits of dual-land use, low-carbon emissions, low maintenance, and is coupled with incentives from governments in countries from around the world. Additionally, agri-photovoltaics provides various agricultural operations that can sustainbly improve crop production by reducing the reliance on non-renewable resources.[63]

Agri-photovoltaic systems can be installed on open-field farms or integrated with protected crop cultivation environments of greenhouses in which the interspace PV is mainly applied in pasture and arable farming, while overhead PV is mainly suitable for horticulture, as shown in Figure 16.[64] The plants under the PV modules benefit from effective water/rain redeployment,[65] wind mitigation and temperature deviation protection,[66] reduction in evapotranspiration, perfection in soil moisture, security in contrast to climatic uncertainty and risky happenings such as hailstones.[67] The first concept of agri-photovoltaic was proposed in 1982 by Goetzberger and Zastrow. They reported that almost the same amount of radiation can be achieved if the collectors are elevated by about 2 m above the ground with the periodic distance between collectors.[68] Recently, literature has introduced an agri-photovoltaic case study in Niger located in West Africa in the Sahel Zone, where the country is exposed to mostly hot and dry desert weather with most of the terrain in desert and sand dunes. With the estimated 23 million population, but only 17% living in urban area who have higher opportunity for access to safe drinking water,[69] this country urgently needs a sustainable development in energy and food generation. The results show that the combination of solar energy for use with food production and water supply by implementing agri-photovoltaic is promising in the villages in Niger. By now, the largest agri-photovoltaic research facility has been installed by Fraunhofer ISE near Lake Constance with a capacity of 194.4 kW in Germany.[70] More and more countries encourage agri-photovoltaics from the perspective of policy and financial subsidies. However, agri-photovoltaics is still in its infancy with insufficient details on the performance of crops and energy generation, the effect of module types, tilt angle, orientation and different types of crops. Moreover, additional investigations in practical business use between local farmers, potential investors and traders, and case studies in different countries are also needed.

Figure 16 The demonstration of (a) Elevated agri-photovoltaic plant, (b) tunnel types greenhouses agri-photovoltaic and (c) and (d) Orchard Agri-photovoltaic plant .The figure is regenerated from Ref.[71]

Disturbance and impacts on the environments with the solar panel/power developments

Solar energy is naturally abundant and environmentally sustainable energy than the combustion of fossil fuel energy sources; further, the use of solar energy reduces the amount of greenhouse gases and air pollution. However, there are some drawbacks associated with the use of solar energy; these include the disturbance to the land and eco-life, and the impact to the soil, water, and air.

The construction of concentrated solar facilities requires large areas of land which may lead to interference with grazing, agriculture use or other business utilities. Thus, it is necessary to have proper policy coordinates with the ability to make informed decisions; this is particularly important in determining the location of concentrated solar facilities to largely prevent the disturbance of land use. In recent years, several state-of-the-art-technologies have been proposed to prevent land disturbance such as floating solar farms on reservoirs,[72] partial-shading on agriculture,[73] mounting solar panels on buildings & roof tops and siting on degraded lands.[74] In 2021, McKuin et al reported the use of cadmium telluride (CdTe) solar-power panels over canals which can effectively generate electricity and reduce the amount of water from evaporation at a reasonable cost.[75] This plan will tackle the problem that conventional on-ground solar may disturb the working and useful agricultural lands. At the same time, problems of bird mortality and loss of wildlife habitat due to deforestation are minimized. Although the water use per unit of generation of solar power is less than many other energy technologies (0.02 m^3 MW h^{-1}), due to their size, they can utilize substantial amounts of water for construction and operation, mostly for cleaning PV solar panels and for dust suppression from disturbed soils.[76,77] Parabolic trough and central tower systems typically use conventional steam plants to generate electricity, which commonly consume water for cooling.[77]

Besides the above-mentioned problems, the impacts to the surrounding animals and biodiversity with the use of solar energy are the predominant problems with renewable energy developments. Large areas of land are currently being evaluated for utility-scale solar energy development (USSED) including areas with high biodiversity and protected species.[78] It has been reported that PV panels with a 10% conversion efficiency would need to cover an area of about 32,000 square kilometers, or approximately area close to the state of Maryland.[79] These activities involve significant ground disturbance

Citation: Lin L, Bora B, Prasad B, et al. Influence of outdoor conditions on PV module performance – an overview. *Material Sci & Eng*. 2023;7(2):88–101. DOI: 10.15406/mseij.2023.07.00210

and have direct (e.g., mortality) and indirect (e.g., habitat loss, degradation, modification) impacts on wildlife and their habitat.[80] For example, the potential impacts on deer, sheep and even the tortoises in the desert include the impediments to free movement, the creation of migration bottlenecks and a reduction in effective winter range size.[78] Moreover, the fans and pumps that are associated with the cooling systems in the solar power developments generate noise which may cause hearing loss in animals and interfere with the ability to hunt. Last but not the least, the alteration of landscape potentially creates microclimate effects which may change the characteristics of the environment that affects the wildlife. For example, the unused heat surrounding the concentrating solar power facilities may damage the wildlife by creating localized drought or high temperature conditions. To minimize biodiversity risks, solar project developers should avoid areas of high environmental significance such as protected areas and conserve areas according to the guidelines.[81–93]

Conclusion

This review presents a comprehensive study on the influence of outdoor conditions on the performance of solar panels. Detailed realization of the module performance under low light intensity gives an insight into the processes and factors affecting device performance. Changing light intensity not only changes the photo-generated current density, but also has a significant impact on the PV performance parameters. It has been observed that when the PV module is exposed to high RH condition, the moisture will penetrate into the solar cell which leads to the delamination and corrosion to the encapsulant. The shade loss and hot-spot tolerance of solar cell modules and the strategy to mitigate these problems is briefly discussed.

The results from the literature show that perovskites and perovskite based solar cells exhibit excellent particle radiation tolerance than most of the types solar cells due to their large carrier diffusion length. Besides, they are not only good candidates for space applications, but also have high thermal stability and *PCE* for terrestrial applications. By realizing the relationship between humidity, irradiance and particle radiation and their relationship with PV parameters, the user could have an improved design for future PV modules, especially, for space applications. A brief introduction to CSP, agri-photovoltaics and the impact on livestock and farm land is presented.

Acknowledgments

None.

Funding

None.

Conflicts of interest

There are no conflicts of interest.

References

1. Bora B, Sastry OS, Kumar A, et al. Estimation of most frequent conditions and performance evaluation of three photovoltaic technology modules. *Journal of Solar Energy Engineering*. 2016;138(5):054504.
2. Cornaro C, Musella D. Comparative analysis of crystalline and double-junction amorphous silicon modules performance in outdoor conditions. *Journal of Solar Energy Engineering*. 2013;135(3):031022.
3. Ishii T, Otani K, Itagaki A, et al. A Methodology for estimating the effect of solar spectrum on photovoltaic module performance by using average photon energy and a water absorption band. *Japanese Journal of Applied Physics*. 2012;51(10S):10NF05.
4. Terrestrial photovoltaic (PV) modules - Design qualification and type approval - Part 1-1: special requirements for testing of crystalline silicon photovoltaic (PV) modules. 2016.
5. Photovoltaic (PV) module performance testing and energy rating - Part 1: Irradiance and temperature performance measurements and power rating. 2011.
6. Duffie J, Beckman W. Solar engineering of thermal processes; John Wiley & Sons, Inc; 1991.
7. King DL, Kratochvil JA, Boyson WE. Measuring solar spectral and angle-of-incidence effects on photovoltaic modules and solar irradiance sensors. Twenty Sixth IEEE Photovoltaic Specialists Conference. 1997. p. 1113–1116.
8. Magare DB, Sastry OS, Gupta R, et al. Effect of seasonal spectral variations on performance of three different photovoltaic technologies in India. *International Journal of Energy and Environmental Engineering*. 2016;7(1):93–103.
9. Photovoltaic devices - Part 3: Measurement principles for terrestrial photovoltaic (PV) solar devices with reference spectral irradiance data; 2019
10. Photovoltaic devices – Procedures for temperature and irradiance corrections to measured I-V characteristics. 2009.
11. Singh P, Ravindra N. Temperature dependence of solar cell performance - an analysis. *Solar Energy Materials and Solar Cells*. 2012;101:36–45.
12. Lin L, Ravindra NM. Temperature dependence of CIGS and perovskite solar cell performance: an overview. *SN Applied Sciences*. 2020;2(8):1361.
13. Buday M. Measuring irradiance, temperature, and angle incidence effects on photovoltaic modules in Auburn hills, Michigan; 2011.
14. Hishikawa Y, Tobita H, Sasaki A, et al. Current-voltage characteristics of novel PV devices under various irradiance and temperature conditions. IEEE 39th Photovoltaic Specialists Conference (PVSC); June 16–21. 2013. p. 1417–1422.
15. Li Q, Shen K, Yang R, et al. Comparative study of GaAs and CdTe solar cell performance under low-intensity light irradiance. *Solar Energy*. 2017;157:216–226.
16. Bashir MA, Ali HM, Khalil S, et al. Comparison of performance measurements of photovoltaic modules during winter months in Taxila, Pakistan. *International Journal of Photoenergy*. 2014;2014:898414.
17. Sumaryada T, Rohaeni S, Damayanti NE, at al. Simulating the performance of $Al_{0.3}Ga_{0.7}As$/InP/Ge multijunction solar cells under variation of spectral irradiance and temperature. *Modelling and Simulation in Engineering*. 2019;2019:5090981.
18. Tress W, Domanski K, Carlsen B, et al. Performance of perovskite solar cells under simulated temperature-illumination real-world operating conditions. *Nature Energy*. 2019;4(7):568–574.
19. Al-Saleem H, Kasim N, Abed A. Efficiency and performance improvement via using optical reflectors of on-grid CIGS PV solar system. *The Karbala International Journal of Modern Science*. 2020;6(1):5.
20. Song Z, Abate A, Watthage SC, et al. Solar cell stability in humid air: partially reversible phase transitions in the PbI2-CH3NH3I-H2O system. *Advanced Energy Materials*. 2016;6(19):1600846.
21. Tan CM, Chen BKE, Toh KP. Humidity study of a-Si PV cell. *Microelectronics Reliability*. 2010;50(9–11):1871–1874.
22. Manoj Kumar Panjwani Ghous Bukshsh Narejo. Effect of humidity on the efficiency of solar cell (photovoltaic). *International Journal of Engineering Research and General Science*. 2014;2(4):499–503.
23. Mekhilef S, Saidur R, Kamalisarvestani M. Effect of dust, humidity and air velocity on efficiency of photovoltaic cells. *Renewable and Sustainable Energy Reviews*. 2012;16(5):2920–2925.

24. Rahman MM, Hasanuzzaman M, Rahim NA. Effects of various parameters on PV-module power and efficiency. *Energy Conversion and Management*. 2015;103:348–358.

25. Tariq Ahmed Hamdi R, Abdulhadi S, Kazem HA, et al. Humidity impact on photovoltaic cells performance: A review; 2018.

26. Chaichan M. Effect of humidity on the PV performance in Oman. *Asian Transactions on Engineering*. 2012;2:29–32.

27. Bhatt P, Kumar M, Chandra Kant P, et al. Optoelectronic modelling of perovskite solar cells under humid conditions and their correlation with power losses to quantify material degradation. *Organic Electronics*. 2016;39:258–266.

28. Sugiyama M, Yasuniwa T, Nakanishi H, et al. Optical and solar cell properties of alpha-ray, proton, and gamma-ray irradiated Cu(In,Ga) Se_2 thin films and solar cells. *Japanese Journal of Applied Physics*. 2010;49(4):042302.

29. Brus VV, Lang F, Bundesmann J, et al. Defect dynamics in proton irradiated CH3NH3PbI3 perovskite solar cells. *Advanced Electronic Materials*. 2017;3(2):1600438.

30. Miyazawa Y, Ikegami M, Miyasaka T, et al. Evaluation of radiation tolerance of perovskite solar cell for use in space. 2015.

31. Guanggen, Z, Xulin H, Bing l, et al. The effect of irradiation on the mechanism of charge transport of CdTe solar cell. 2013.

32. Pons D, Bourgoin JC. Irradiation-induced defects in GaAs. *Journal of Physics C: Solid State Physics*. 1985;18(20):3839–3871.

33. Tada HYC, Anspaugh BE, Downing RG. Solar cell radiation handbook; National Aeronautics and Space Administration; California Institute of Technology. 1982.

34. Lang F, Jošt M, Bundesmann J, et al. Efficient minority carrier detrapping mediating the radiation hardness of triple-cation perovskite solar cells under proton irradiation. *Energy & Environmental Science*. 2019;12(5):1634–1647.

35. Lang F, Jošt M, Frohna K, et al. Proton Radiation Hardness of Perovskite Tandem Photovoltaics. *Joule*. 2020; 4(5):1054–1069.

36. Espinet-Gonzalez P, Barrigón E, et al. Radiation tolerant nanowire array solar cells. *ACS Nano*. 2019;13 (11):12860–12869.

37. Miyazawa Y, Ikegami M, Chen HW, et al. Tolerance of perovskite solar cell to high-energy particle irradiations in space environment. *iScience*. 2018;2:148–155.

38. Bätzner DL, Romeo A, Zogg H, et al. Development of efficient and stable back contacts on CdTe/CdS solar cells. *Thin Solid Films*. 2001;387(1–2):151–154.

39. Cho S, Ahn SH, Cho IJ, et al. Radiation hardness of cadmium telluride solar cells in proton therapy beam mode. *PLOS ONE*. 2019;14(9):e0221655.

40. Lang F, Nickel NH, Bundesmann J, et al. Radiation hardness and self-healing of perovskite solar cells. *Advanced Materials*. 2016;28(39):8726–8731.

41. Huang JS, Kelzenberg M, Espinet-González P, et al. Effects *of Electron and Proton Radiation on Perovskite Solar Cells for Space Solar Power Application*. 2017.

42. Yamaguchi M, Taylor SJ, Matsuda S, et al. Mechanism for the anomalous degradation of Si solar cells induced by high fluence 1 MeV electron irradiation. *Applied Physics Letters*. 1996;68(22):3141–3143.

43. Cho B, Davis J, Hise L, et al. Qualification testing of the ZTJ GaInP2/GaInAs/Ge solar cell to the AIAA S-111 standard. 34th IEEE Photovoltaic Specialists Conference (PVSC);2009 June 7–12; 2009. p. 001009–001014.

44. Jasenek A, Rau U. Defect generation in Cu(In,Ga)Se_2 heterojunction solar cells by high-energy electron and proton irradiation. *Journal of Applied Physics*. 2001;90(2):650–658.

45. Bätzner D, Romeo A, Zogg H, et al. Radiation Hardness of CdTe/CdS solar cells. 2001.

46. Anspaugh BE. GaAs Solar cell radiation handbook; Jet Propulsion Laboratory, California Institute of Technology Pasadena, California, USA; 1996.

47. Sullivan RM. Shadow effects on series-parallel array of solar cells; NASA-TM-X-55269, X-636-65-207, NASA, NASA Goddard Space Flight Center; Greenbelt, MD, United States; 1965.

48. Zhang J, Wu X, Song, M, et al. An effective method for hot spot temperature optimization in heat conduction problem. *Applied Thermal Engineering*. 2023;227:120325.

49. Li G, Wang F, Feng F, et al. Hot spot detection of photovoltaic module based on distributed fiber bragg grating sensor. *Sensors*. 2022;22(13):4951.

50. Akbari M, Mostafaei M, Rezaei-Zare A. Estimation of hot-spot heating in OIP transformer bushings due to geomagnetically induced current. *IEEE Transactions on Power Delivery*. 2023;38(2):1277–1285.

51. Wu Z, Hu Y, Wen JX, et al. A review for solar panel fire accident prevention in large-scale PV applications. *IEEE Access*. 2020;8:132466–132480.

52. Bowring AR, Bertoluzzi L, O'Regan BC, et al. Reverse bias behavior of halide perovskite solar cells. *Advanced Energy Materials*. 2018;8(8):1702365.

53. Yang H, Wang H, Wang M. Investigation of the relationship between reverse current of crystalline silicon solar cells and conduction of bypass diode. *International Journal of Photoenergy*. 2012;2012:357218.

54. Khodapanah M, Ghanbari T, Moshksar E, et al. Partial shading detection and hotspot prediction in photovoltaic systems based on numerical differentiation and integration of the P − V curves. *IET Renewable Power Generation*. 2023;17(2):279–295,

55. Wolf EJ, Gould IE, Bliss LB, et al. Designing modules to prevent reverse bias degradation in perovskite solar cells when partial shading occurs. *Solar RRL*. 2022;6(3):2100239.

56. Lamb WP, Asnes DE, Kupfer J, et al. Real-Time anticipation and prevention of hot spots by monitoring the dynamic conductance of photovoltaic panels. *IEEE Journal of Photovoltaics*. 2022;12(4):1051–1057.

57. Teo JC, Tan R, Mok VH, et al. Effects of bypass diode configurations to the maximum power of photovoltaic module. *International Journal of Smart Grid and Clean Energy*. 2017;6:225–232

58. Vieira RG, Dhimish M, Guerra MIS, et al. A comprehensive review on bypass diode application on photovoltaic modules. *Energies*. 2020;13(10):2472.

59. Shin WGK, Song HJ, Ju YC, et al. Origin of bypass diode fault in c-si photovoltaic modules: leakage current under high surrounding temperature. *Energies*. 2018;11(9):2416.

60. Silvestre S, Boronat A, Chouder A. Study of bypass diodes configuration on PV modules. *Applied Energy*. 2009;86(9):1632–1640.

61. Bana S, Saini RP. Experimental investigation on power output of different photovoltaic array configurations under uniform and partial shading scenarios. *Energy*. 2017;127:438–453.

62. Kaid IE, Hafaifa A, Guemana M, et al. Photovoltaic system failure diagnosis based on adaptive neuro fuzzy inference approach: South Algeria solar power plant. *Journal of Cleaner Production*. 2018;204:169–182.

63. Niazi KA, Akhtar W, Khan HA, et al. Hotspot diagnosis for solar photovoltaic modules using a Naive Bayes classifier. *Solar Energy*. 2019;190:34–43.

64. Dhimish M, Holmes V, Mehrdadi B, et al. PV output power enhancement using two mitigation techniques for hot spots and partially shaded solar cells. *Electric Power Systems Research*. 2018;158:15–25.

Citation: Lin L, Bora B, Prasad B, et al. Influence of outdoor conditions on PV module performance – an overview. *Material Sci & Eng*. 2023;7(2):88–101.
DOI: 10.15406/mseij.2023.07.00210

65. Dhimish M, Badran G. Current limiter circuit to avoid photovoltaic mismatch conditions including hot-spots and shading. *Renewable Energy.* 2020;145:2201–2216.

66. Afridi M, Kumar A, Ibne Mahmood F, at al. Hotspot testing of glass/backsheet and glass/glass PV modules pre-stressed in extended thermal cycling. *Solar Energy*. 2023;249:467–475.

67. Agency IE. Technology roadmap—solar thermal electricity. Technology report. Paris: International Energy Agency. 2014.

68. 2022 Grand View Research, I. Concentrated solar power market size, share & trends analysis report by application (utility, EOR, desalination), by technology, by region, and segment forecasts. 2020.

69. Ding W, Bauer T. Progress in research and development of molten chloride salt technology for next generation concentrated solar power plants. *Engineering.* 2021;7(3):334–347.

70. Mutaz B, Elbeh AKS. Analysis and optimization of concentrated solar power plant for application in arid climate. *Energy Science and Engineering;* 2021;9(6):784–797.

71. Zayed ME, Zhao J, Elsheikh AH, et al. A comprehensive review on Dish/Stirling concentrated solar power systems: Design, optical and geometrical analyses, thermal performance assessment, and applications. *Journal of Cleaner Production*. 2021;283:124664.

72. Mehos M, Turchi, Craig, et al. Concentrating Solar Power Gen3 Demonstration Roadmap. 2017.

73. Gorjian S, Minaei S, Maleh Mirchegini L, et al. Applications of solar PV systems in agricultural automation and robotics. In: Gorjian S, Shukla A, Editors. *Photovoltaic Solar Energy Conversion*. Academic Press; 2020. p. 191–235.

74. Gorjian S, Ebadi, H, Najafi, et al. Recent advances in net-zero energy greenhouses and adapted thermal energy storage systems. *Sustainable Energy Technologies and Assessments.* 2021;43:100940.

75. Gorjian S, Bousi E, Özdemir OE, et al. Progress and challenges of crop production and electricity generation in agrivoltaic systems using semi-transparent photovoltaic technology. *Renewable and Sustainable Energy Reviews*. 2022;158:112126.

76. Amaducci S, Yin X, Colauzzi M. Agrivoltaic systems to optimise land use for electric energy production. *Applied Energy*. 2018;220:545–561.

77. Marrou H, Guilioni L, Dufour L, et al. Microclimate under agrivoltaic systems: Is crop growth rate affected in the partial shade of solar panels? *Agricultural and Forest Meteorology*. 2013;177:117–132.

78. Marrou H, Dufour L, Wery J. How does a shelter of solar panels influence water flows in a soil–crop system? *European Journal of Agronomy*. 2013;50:38–51.

79. Goetzberger A, Zastrow A. On the coexistence of solar-energy conversion and plant cultivation. *International Journal of Solar Energy*. 1982;1(1):55–69.

80. Neupane Bhandari S, Schlüter S, Kuckshinrichs W, et al. Economic feasibility of agrivoltaic systems in food-energy nexus context: modelling and a case study in niger. *Agronomy.* 2021;11(10):1906.

81. Trommsdorff M, Kang J, Reise C, et al. Combining food and energy production: design of an agrivoltaic system applied in arable and vegetable farming in Germany. *Renewable and Sustainable Energy Reviews.* 2021;140:110694.

82. ISE F. Agri-photovoltaics, opportunity for agriculture and energy transition. 2020.

83. Pimentel Da Silva GD, Branco DAC. Is floating photovoltaic better than conventional photovoltaic? Assessing environmental impacts. *Impact Assessment and Project Appraisal.* 2018;36(5):390–400.

84. Ravi S, Macknick J, Lobell D, et al. Colocation opportunities for large solar infrastructures and agriculture in drylands. *Applied Energy.* 2016;165:383–392.

85. Niblick B, Landis AE. Assessing renewable energy potential on United States marginal and contaminated sites. *Renewable and Sustainable Energy Reviews*. 2016;60:489–497.

86. McKuin B, Zumkehr A, Ta J, et al. Energy and water co-benefits from covering canals with solar panels. *Nature Sustainability*. 2021;4(7):609-617.

87. Ravi S, Lobell DB, Field CB. Tradeoffs and Synergies between biofuel production and large solar infrastructure in deserts. *Environ Sci Technol*. 2014;48(5):3021–3030.

88. Hernandez RR, Hoffacker MK, Field CB. Land-use efficiency of big solar. *Environmental Science & Technology*. 2014;48(2):1315–1323.

89. Burkhardt JJ, Heath GA, Turchi CS. Life cycle assessment of a parabolic trough concentrating solar power plant and the impacts of key design alternatives. *Environmental Science & Technology*. 2011;45(6):2457–2464.

90. Lovich JE, Ennen JR. Wildlife conservation and solar energy development in the desert southwest, United States. *BioScience.* 2011;61(12):982–992.

91. Wilshire HG, Hazlett RW. The American west at risk: science, myths, and politics of land abuse and recovery; Oxford University Press; 2008.

92. William PK, Leonard AB, Michael LM, et al. Wind energy development and wildlife conservation: challenges and opportunities. *Journal of Wildlife Management*. 2007;71(8):2487–2498.

93. Wilson D, Phair N, Carbone, et al. Mitigating biodiversity impacts associated with solar and wind energy development: guidelines for project developers; IUCN, Global Business and Biodiversity Program, The Biodiversity Consultancy. 2021.

Citation: Lin L, Bora B, Prasad B, et al. Influence of outdoor conditions on PV module performance – an overview. *Material Sci & Eng*. 2023;7(2):88–101.
DOI: 10.15406/mseij.2023.07.00210